energies

MDPI

Article

Efficiency Enhancement of Tilted Bifacial Photovoltaic Modules with Horizontal Single-Axis Tracker—The Bifacial Companion Method

Shitao Wang [1,2], Yi Shen [1,*], Junbing Zhou [2], Caixia Li [2] and Lijun Ma [2]

[1] Department of Control Science and Engineering, Harbin Institute of Technology, Harbin 150001, China; brucewang@hitwh.edu.cn

[2] Arctech Solar Technology Limited Holdings, Kunshan 215331, China; casren.zhou@arctechsolar.com (J.Z.); sherry.li@arctechsolar.com (C.L.); Mia.ma@arctechsolar.com (L.M.)

* Correspondence: shen@hit.edu.cn; Tel.: +86-451-864-13411-8602; Fax: +86-451-864-18378

Abstract: Bifacial photovoltaic modules combined with horizontal single-axis tracker are widely used to achieve the lowest levelized cost of energy (LCOE). In this study, to further increase the power production of photovoltaic systems, the bifacial companion method is proposed for light supplementation and the efficiency enhancement of tilted bifacial modules with a horizontal single-axis tracker. Specifically, a solar reflector is added to the rear end of the tilted bifacial photovoltaic module to guide the sunlight and promote power generation on the rear end. The technical feasibility of the proposed method is verified through optimal calculation and prototype experimental test. The theoretical calculation results suggest that the bifacial companion system is particularly suitable for mid-to-high latitude areas. The higher the latitude, the higher the gain ratio of generated power in the system; there is an optimal module tilt angle that maximizes the efficiency at different latitudes. The closer the module tilt angle to the optimal tilt angle, the higher the power generation efficiency of the system. Meanwhile, compared to the fixed solar reflector, the use of tracking solar reflector is more conducive to improving the power generation efficiency of the system. For the 37.5° latitude area, the annual average power generation gain ratio of the bifacial companion system with tracking solar reflector and fixed solar reflector can reach up to 30% and 17%, respectively. Additionally, the test results for the three sets of bifacial companion prototypes (module tilt angles of 10°, 20°, and 30°) with a fixed solar reflector show that the maximum gain ratio of daily power generation in August 2021 are 8.2%, 13%, and 18.1%, and that in September 2021 are 7%, 8.7% and 13.7%, respectively, which are consistent with the theoretical results.

Keywords: tilted horizontal single-axis tracker; photovoltaic support system; bifacial photovoltaic module; bifacial companion; fixed/tracking solar reflector; light supplementation and efficiency enhancement

Citation: Wang, S.; Shen, Y.; Zhou, J.; Li, C.; Ma, L. Efficiency Enhancement of Tilted Bifacial Photovoltaic Modules with Horizontal Single-Axis Tracker—The Bifacial Companion Method. *Energies* **2022**, *15*, 1262. https://doi.org/10.3390/en15041262

Academic Editor: Tapas Mallick

Received: 11 January 2022
Accepted: 7 February 2022
Published: 9 February 2022

1. Introduction

With the rapid development of the photovoltaic power generation industry, the demand for efficiency enhancement and cost reduction is continuously increasing. The main factors affecting the efficiency and cost of photovoltaic power generation systems are solar resources at the project site, photovoltaic module characteristics (efficiency, bifacial factor), photovoltaic support form, additional irradiation, etc. [1]. These aspects have garnered extensive research attention in the recent years.

Firstly, bifacial photovoltaic modules [2] are becoming increasingly popular because they can transform solar radiation into electricity from both front and rear sides. Compared to a monofacial photovoltaic module, the power generation of a bifacial photovoltaic module is higher by approximately 10–40% on a global scale [3–6]. Further, the photoelectric conversion efficiency of the front and rear sides of a bifacial photovoltaic module has been improving year by year. The front efficiency of single-crystal passivated emitter and rear

contact (PERC) solar cell has exceeded 22%; the bifacial factor has reached nearly 80%; and the bifacial factor of heterojunction (HJT) and n-type passivated emitter rear totally diffused (n-PERT) battery technology can reach more than 90% [7–11]. The maturity of bifacial photovoltaic module technology has paved the way for its large-scale industrial application in the field of solar energy. In 2019, 5 GW of bifacial photovoltaics were installed worldwide [12]; the international photovoltaic technology road map (ITRPV) in 2020 [13] predicts that bifacial solar cells will soon dominate the market, and the global market share of crystalline silicon (c-Si) bifacial photovoltaic cells and modules will exceed 35% by 2028.

Secondly, in addition to the photovoltaic module, the photovoltaic support form has a significant impact on the power generation performance of the system. The photovoltaic module is generally mounted on an appropriate structure, either fixed or with tracking. Among them, fixed mounted structures are divided into horizontal fixed mounted, fixed-tilt mounted, and vertical fixed mounted structures according to different tilt angles [14,15]; trackers are divided into horizontal single-axis tracker, tilted single-axis tracker, horizontal single-axis tracker with tilted module, and dual-axis tracker [16–20]. Trackers can effectively improve the efficiency of power generation. Al-Mohamad [14] found that the daily output power of a single-axis tracking photovoltaic module could be increased by more than 20% in comparison with that of a fixed module. Lazaroiu et al. [15] studied the power generation gain and energy consumption of a photovoltaic system with solar tracking, and the results indicated a significant growth in the power production during morning and evening. Patel et al. [21] showed that when the geographic latitude was lower than 30°, the annual power generation of a single-axis tracking system was higher than that of an optimal fixed-tilt mounted system by 25–45%. Regarding the solar tracking method, based on the traditional maximum power point tracking method (MPPT) [22], Clifford and Eastwood [23] proposed a novel passive solar tracker, whose power generation gain could reach 30%. Fathabadi et al. [24,25] proposed a sensor-less, high-precision dual-axis, closed-loop, solar tracking system, whose power generation gain reached 28–43%.

Due to the excellent characteristics of bifacial modules and solar tracker, the combination of the two can offer unprecedented advantages and has attracted wide attention. The bifacial photovoltaic module is often used in fixed-tilt mounted and tracking configurations. Egido and Lorenzo [26] established a theoretical model to deduce that the annual total energy obtained by a bifacial photovoltaic module with a dual-axis tracker was 80% higher than that obtained by a fixed mounted monofacial photovoltaic module and 30% higher than that obtained by a fixed mounted bifacial photovoltaic module. Gu et al. [27] compared the electrical and thermal performances of bifacial and monofacial photovoltaic modules, and they found that the daily bifacial gains for sunny and cloudy days were 13.08% and 16.54%, respectively. Pelaez et al. [28] observed that the bifacial gain in the single-axis tracking system was 4–15%, and the global average gain was 9%. Sun et al. [3] examined the relationship of bifacial gain with the ground albedo and geographic latitude. The results revealed that, when the ground albedo was less than 25%, the bifacial gain of the bifacial photovoltaic module installed on the ground was less than 10% globally; by increasing the albedo to 50% and raising the module to 1 m above the ground, the bifacial gain could be increased to 30%. Kopecek et al. [6] showed that by using bifacial module in an optimal fixed-tilt mounted system, the annual energy yield could be increased by 30% compared with that of a monofacial module. Furthermore, by combining bifacial modules with single-axis tracking systems, the energy yield was expected to increase by more than 40%.

Additionally, it is possible to increase the power generation of the system by increasing the solar energy received by the module, usually in the form of a diffuse reflection from ground, reflector reflection, and concentrated lens refraction [29]. The ground diffuse reflection depends on the ground conditions. In common natural environments, the albedos of soil, green grass, and concrete are approximately 9%, 23%, and 25%, respectively, while that of fresh snow can exceed 90% [30]. The albedo of different environments varies greatly. Among the active concentration method, the V-groove reflector [31–33] is the most common device to increase the radiation intensity received in front of the module.

Ooshaksaraei et al. [34] tested the power generation after adding semi-mirror and diffuse reflectors at the back surface of a bifacial photovoltaic module and observed an output power enhancement of 20% and 15% from the semi-mirror and diffuse reflectors, respectively. Although the above methods can effectively increase the power generation of the system, the layout of the reflector and the economic problems of the system have not been perfectly resolved yet.

Finally, in terms of the economic efficiency of bifacial photovoltaic modules combined with tracking systems, the bifiPV2020 [12] technical review released by NREL pointed out that for the bifacial module with horizontal single-axis tracker, in the Middle East and North Africa, Chile, and the United States, the list price will soon drop below 10 USD/MWh. Guo et al. [35] compared the vertically mounted photovoltaic modules facing east–west and conventionally mounted traditional mono-facial module, and they found that the pros and cons of the two methods depend on three factors: (i) geographic latitude, (ii) local diffuse reflection coefficient, and (iii) ground albedo. Chudinzow et al. [36] investigated the effects of installation row spacing, the tilt angle of the photovoltaic module, and ground reflectivity on the power generation and the levelized cost of energy (LCOE) of fixed-tilt and single-axis tracked bifacial photovoltaic modules. Patel et al. [37] found that for systems with module-related costs higher than land-related costs and project latitude higher than 30°, the tilt angle of bifacial photovoltaic modules is 10°–45°, and the LCOE can be reduced by 2–6%. Riedel-Lyngskær et al. [38] pointed out that, compared to the optimal fixed-tilt mounted system, a horizontal single-axis tracker system can reduce the LCOE by 3.5 EUR/MWh, and a bifacial photovoltaic module can reduce LCOE by 4.0 EUR/MWh. Furthermore, the high cost and structural complexity have limited the wide application of dual-axis tracker.

To recapitulate, bifacial photovoltaic modules combined with single-axis trackers are a widely utilized technology to minimize the LCOE. However, this technology has the potential for further improvement. For instance, the rear of a bifacial photovoltaic module only passively receives ambient scattered light and ground diffuse reflection light. Further, its power generation efficiency is affected by environmental factors, such as ground albedo. Therefore, the rear power generation gain can be increased by further optical optimization. Consequently, how to combine the existing support technology to further improve the power generation efficiency on the rear side of the bifacial photovoltaic module is an important research direction, which can boost the development of photovoltaic industry. To address this issue, in this study, the bifacial companion method is proposed for light supplementation and efficiency enhancement of tilted bifacial modules with a horizontal single-axis tracker. Specifically, this method can increase the radiation intensity on the rear side of the module, thereby improving the power generation efficiency.

2. Principle of the Proposed Bifacial Companion Method

The bifacial companion method is based on the principle that for the horizontal single-axis tracker of the existing tilted module (the tracking axis is north–south NS), glass solar reflectors and other sunlight reflecting devices can be introduced in the gaps between adjacent modules to reflect the received sunlight in these gaps to the rear side of the bifacial photovoltaic module. The bifacial companion is an innovative module radiation enhancement method, which is different from the existing solar photovoltaic application technologies. It combines the existing tracking bracket technology with low-power concentration technology and new bifacial module technology. This method can further stimulate the power generation potential of the bifacial photovoltaic module to improve the power generation efficiency and reduce the cost of the system. The principle is shown in Figure 1.

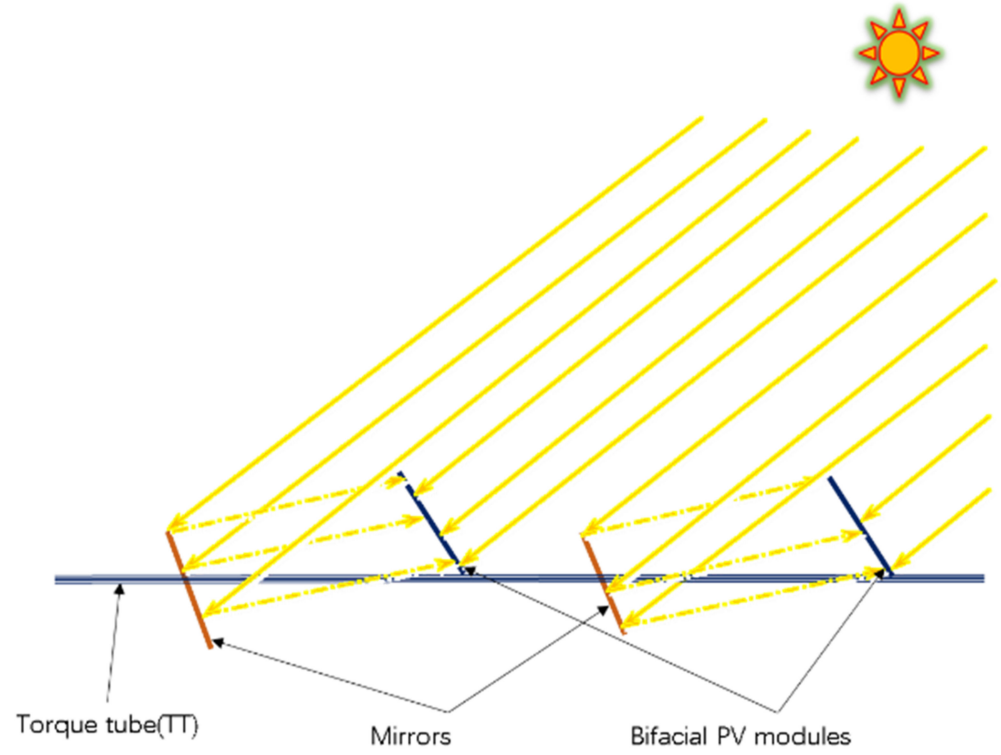

Figure 1. The principle of the bifacial companion method for light supplementation and efficiency enhancement of tilted bifacial modules with horizontal single-axis trackers.

The bifacial companion system mainly includes bifacial photovoltaic module, solar reflector, solar reflector transmission drive device, spindle transmission drive device, and support structure composed of support column (referred to as POST) and rotating spindle (referred to as torque tube), and the rotating spindle can rotate around its axis, as shown in Figure 2. The solar reflector and bifacial photovoltaic module are installed on the support system formed by the support column and spindle. The module is fixed on the spindle with a specific tilt angle (α), and the solar reflector is installed on the spindle structure behind the rear of the module (distance d) through its central axis. The solar reflector can be divided into fixed and tracking according to whether it can rotate around its central axis. The fixed solar reflector is installed on the spindle at a fixed angle (β) and remains unchanged, while the tracking solar reflector can rotate around its central axis to keep track of the Sun's position and reflect the sunlight in the module gap (D) in real time to the designated position on the rear side of the module.

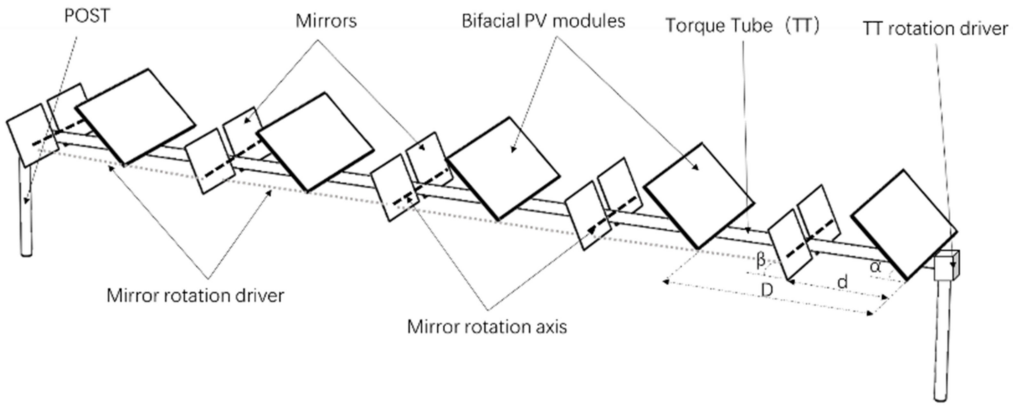

Figure 2. Schematic diagram of the structural composition for light supplementation and efficiency enhancement of tilted bifacial modules with horizontal single-axis trackers.

3. Calculation Method for Design Optimization

The introduction of solar reflector causes the bifacial companion system to become a photovoltaic support with the highest comprehensive power generation efficiency. Meanwhile, the bifacial companion system also acts as an optical system sensitive to the structural size. For parameters of different modules and project sites, the tilt angle of the module and the selection of shape, position, size, and tilt angle of the solar reflector govern the pros and cons of the scheme. Therefore, the key to the design of the bifacial companion system is that, under the conditions of known latitudes of project sites (φ), light resource parameters (GHI = global horizontal irradiance; DHI = diffuse horizontal irradiance; DNI = direct normal irradiance), photovoltaic module size (L × B), front and rear power generation efficiency (front power generation efficiency: λ, module bifacial factor: μ), and other characteristic parameters, the optimal parameter combination (α, β, D, d, l, h) should be obtained, as shown in Figure 3.

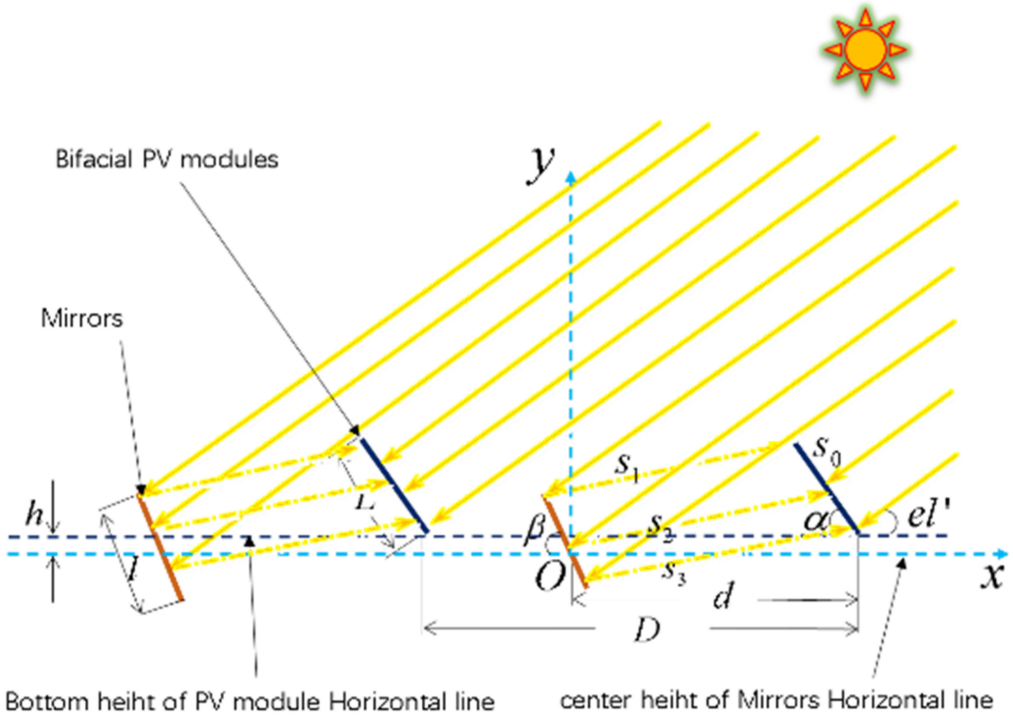

Figure 3. Key parameters of the bifacial companion design.

* Symbol description:

λLocal coordinate system OXY: a coordinate system with the midpoint of solar reflector as the origin, main axis of tracking support as the X axis, and normal of the module installation plane (the surface of the bracket purlin) as the Y axis;

λL: horizontal length of the module;

λl: horizontal length of the solar reflector;

λd: distance between the module and solar reflector;

λD: distance between adjacent modules;

λh: distance between the bottom line of module and the center line of solar reflector;

λα: tilt angle of the module, i.e., the angle between the module section and OX axis;

λβ: tilt angle of the solar reflector, i.e., the angle between solar reflector section and OX axis;

λel': the elevation angle of the Sun relative to the module installation plane, i.e., the angle between the Sun's rays and OX axis;

λS_0: module section line;

λS_1, S_2, S_3: reflected sunlight at the upper edge, center line, and unobstructed bottom of the solar reflector.

3.1. Basic Assumptions and Limitations of the Established Computational Model

3.1.1. Basic Assumptions in the Computational Model

(1) It is assumed that the direct sunlight is parallel light, and the reflection of sunlight from the mirror surface is specular reflection.
(2) The direct solar radiation intensity (*DNI*) is approximately proportional to the solar elevation angle, i.e., $DNI \propto \sin(el)$ This law is based on Iqbal Model C and ASHRAE model [39].
(3) The power generated on the front and back sides of the bifacial module is proportional to the total amount of solar light energy received on the corresponding surface, and the proportionality coefficient is the photoelectric conversion efficiency on each side.

3.1.2. Limitations of the Computational Model

(1) The calculation model only considers the influence of direct sunlight and does not consider scattered light.
(2) The possible power loss caused by the uneven distribution of reflected sunlight (direct sunlight) on the back of the module is not considered in the model.

The above assumptions and limitations may lead to some differences between theoretical and experimental results.

3.2. Calculation Process

The calculation process for obtaining the optimal optical design of bifacial companion system is shown in Figure 4.

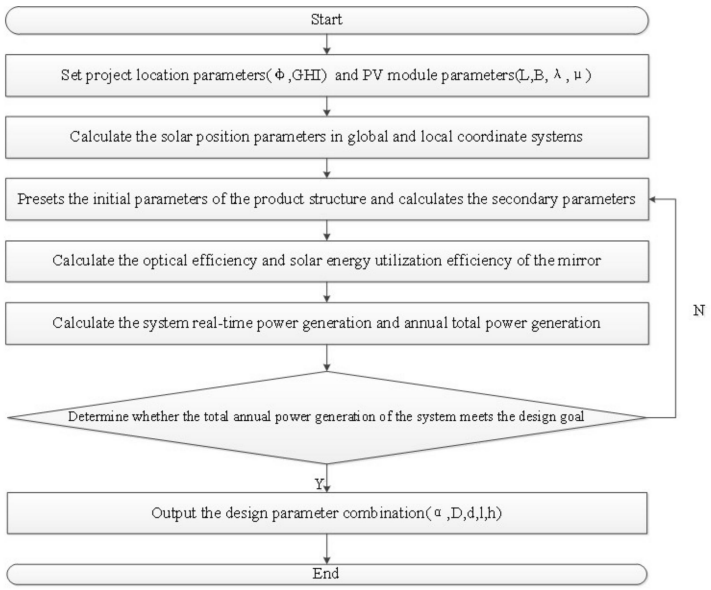

Figure 4. Calculation process for the design optimization of the bifacial companion system.

3.3. Calculation Steps

3.3.1. Setting Basic Parameters

The basic initial parameters include the latitude of project site and solar radiation intensity GHI, DHI, module size, front power generation efficiency λ of the module, bifacial factor μ, etc. These initial parameters are listed in Table 1.

Table 1. Basic parameters of the calculation model.

Object	Parameter	Numerical Value
Module parameters [40]	Specification (B × L × t; mm^3)	2256 × 1133 × 35
	Front power generation efficiency λ	20%
	Bifacial factor μ	75%
Project site parameters	Latitude φ	5–55°
	Solar radiation GHI ($kWh/m^2/year$)	2000
	Solar radiation DHI ($kWh/m^2/year$)	400

3.3.2. Calculation of Solar Position Parameters

(1) Solar position parameters of the global coordinate system

Introducing time parameters (T, N), in the astronomical geocentric celestial coordinate system (see Figure 5a), the approximate equation [41] is used to calculate the solar hour angle $\omega = 15^o \times (T - 12)$, declination angle $\delta = 23.45^o \times \sin\left[\frac{360^o}{365} \times (N + 284)\right]$ at any time, where T is the true solar time and N is the serial number of a day in a year. The solar elevation angle el and azimuth angle az are expressed as follows:

$$\begin{cases} \sin(el) = \sin\varphi \sin\delta + \cos\varphi \cos\delta \cos\omega \\ \sin(az) = \frac{\cos\delta \sin\omega}{\cos(el)} \end{cases} \quad (1)$$

Note: At position O on the latitude φ, there is a tracker (blue colored rectangle). ONS is the horizontal coordinate system of this position, where O is the origin and the N and S axes point north and east, respectively.

(2) Solar position parameters of the local coordinate system

The local coordinate system OXYZ is established by taking the real-time position of the installation plane of the tracking support module as the reference plane, and it is obtained by rotating the geocentric celestial coordinate system (O-East-North-UP) in real time around the O–South axis by a certain angle γ, as shown in Figure 5b. Consequently, in the local coordinate system OXYZ, the azimuth angle az' of the Sun is kept as 0, and the position of the Sun in the two coordinate systems satisfies the following coordinate transformation equation:

$$\vec{OP}_1 = \left[iR_j(X,\gamma)\right] \bullet \vec{OP}_0 \Rightarrow \begin{pmatrix} \cos(el')\cos(az') \\ \cos(el')\sin(az') \\ \sin(el') \end{pmatrix} = \begin{bmatrix} 1 & 0 & 0 \\ 0 & \cos\gamma & \sin\gamma \\ 0 & -\sin\gamma & \cos\gamma \end{bmatrix} \begin{pmatrix} \cos(el)\cos(az) \\ \cos(el)\sin(az) \\ \sin(el) \end{pmatrix}$$

Further, the relationship between the elevation angle el', solar azimuth angle, and elevation angle in the geocentric celestial coordinate system is expressed as follows:

$$\cos(el') = \cos(el)\cos(az) \quad (2)$$

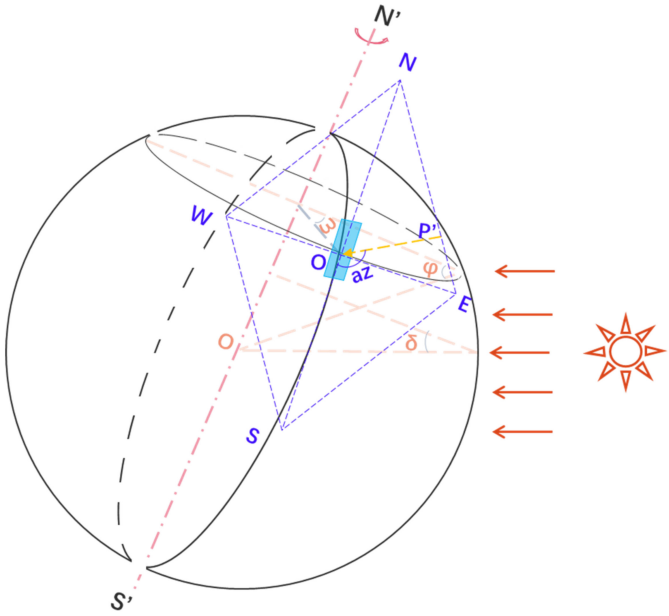

(**a**)

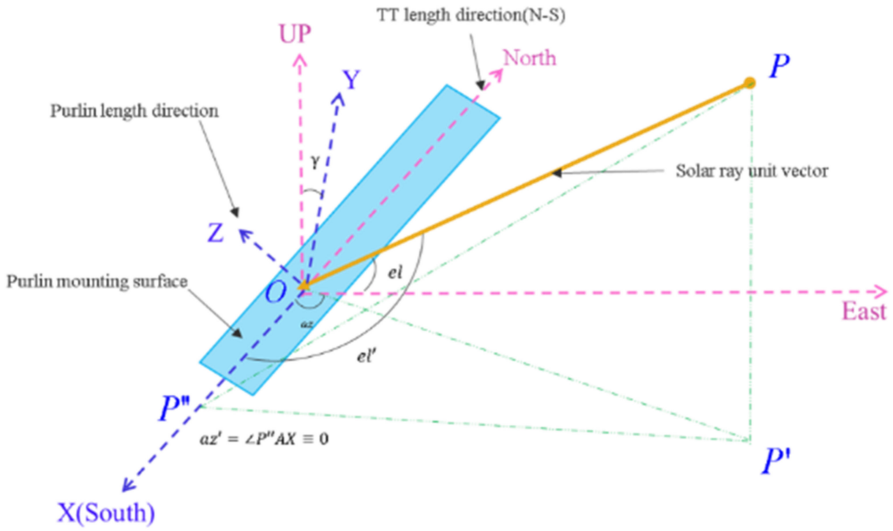

(**b**)

Figure 5. (**a**). Schematic diagram of latitude φ, hour angle ω, declination angle δ, azimuth angle az at any position O on the Earth's surface. (**b**). Local coordinate system OXYZ and geocentric celestial coordinate system.

3.3.3. Introduction of the Initial Variables and Calculation of the Secondary Product Parameters

To obtain the optimal optical design, the initial variable parameters of the structure (α, d, h) are introduced, and the product parameters (D, β, l) are calculated according to the following product design conditions:

(1) Optimal module spacing D: within the designed solar elevation angle range $el' \geq el'_0$, there is no shadow occlusion between the adjacent modules.

$$D = \frac{L \sin(\alpha + el'_0)}{\sin(el'_0)} \tag{3}$$

where el'_0 is the solar altitude angle in the local coordinate system at 9:00 a.m. or 3:00 p.m. on the winter solstice.

(2) Tilt angle β of solar reflector: the center reflection line of the solar reflector always aims at the center of the rear of the module.

$$\beta = \frac{1}{2}a\tan\left(\frac{L\sin\alpha + 2h}{L\cos\alpha - 2d}\right) - \frac{1}{2}el' \tag{4}$$

For fixed reflectors, the reflector tilt angle β is a constant, which is the annual average value of real-time β calculated according to Equation (3).

(3) Optimal horizontal length l of reflector: the solar elevation angle range is $el' \geq el_0$, and the reflector has no shadow at the rear module

$$l \leq 2 \times \frac{Dh + DL\sin\alpha - dL\sin\alpha - hL\cos\alpha}{D\sin\beta + L\cos\beta\sin\alpha - L\cos\alpha\sin\beta} \tag{5}$$

3.3.4. Calculation of Reflector Optical Efficiency

(1) Calculation of occlusion efficiency η_1 of the module to the reflector: occlusion efficiency = 1 − (module shadow length − distance from reflector to module)/reflector shadow length

$$\eta_1 = 1 - \frac{\Delta_L + \left(h + \frac{1}{2}l\sin\beta\right)ctg(el) - \left(d - l\cos\beta\right)}{\Delta_l} \tag{6}$$

(2) Calculation of interception rate η_2 of the reflected light from the reflector by the module: the interception rate is the proportion of reflected light from the reflector projected to the rear side of the module.

First, in the local coordinate system, the coordinates of the intersection of top reflection line $S1$ of the reflector, bottom reflection line $S3$ of the reflector, and truncation line $S0$ of the reflection target are obtained.

$$\begin{aligned} S0 \cap S1 : x_{01} &= \frac{tg\alpha \times d + \frac{1}{2}tg(2\beta+el)l\cos\beta - \frac{1}{2}l\sin\beta + h}{tg\alpha - tg(2\beta+el)} \\ S0 \cap S3 : x_{02} &= \frac{tg\alpha \times d - \left(\eta_1 - \frac{1}{2}\right)tg(2\beta+el)l\cos\beta + \left(\eta_1 - \frac{1}{2}\right)l\sin\beta + h}{tg\alpha - tg(2\beta+el)} \end{aligned} \tag{7}$$

The interception rate of reflected light by the module is expressed as follows:

$$\eta_2 = \frac{x_2 - x_1}{x_{02} - x_{01}} \tag{8}$$

where

$$\begin{aligned} x_2 &= \begin{cases} d - L\cos\alpha & x_{02} \in [-\infty, d - L\cos\alpha] \\ x_{02} & x_{02} \in [d - L\cos\alpha, d] \\ d & x_{02} \in [d, \infty] \end{cases} \\ x_1 &= \begin{cases} d - L\cos\alpha & x_{01} \in [-\infty, d - L\cos\alpha] \\ x_{01} & x_{01} \in [d - L\cos\alpha, d] \\ d & x_{01} \in [d, \infty] \end{cases} \end{aligned} \tag{9}$$

(3) The cosine efficiency η_3 of the reflector to the Sun's incident light is expressed as

$$\eta_3 = \sin(\beta + el') \tag{10}$$

(4) The average reflection efficiency η_4 and reflectivity of the reflector are related to factors, such as the material composition of the reflector and the cleanliness of the reflective surface. In this paper, the annual average reflectivity is taken as a constant: $\eta_4 = 85\%$.

(5) The total optical efficiency η_{sum} of the reflector is the product of each efficiency sub-item of reflected light

$$\eta_{sum} = \prod_i \eta_i \tag{11}$$

The four typical days of the spring equinox, autumnal equinox, summer solstice, and winter solstice are used as calculation time points. Under a known combination of parameters (φ = 37.5, α = 20°, h = 0.4 m, d = D = 1.74 m), the total optical efficiency η_{sum} of the reflector varies with time on four typical days, as shown in Figure 6.

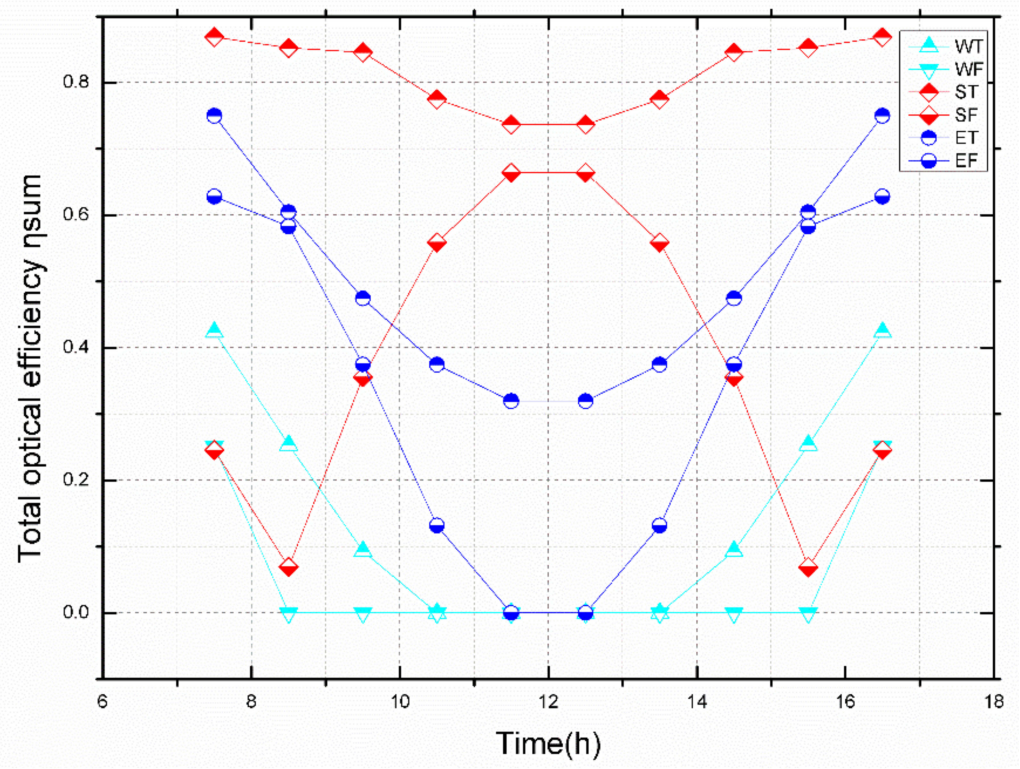

Figure 6. Variation in the reflector optical efficiency with time.

In Figure 6, the labels are a combination of the calculation date and reflector method, such as E—equinox, S—summer, W—winter, T—tracked, and F—fixed. For example, ET represents the efficiency of the tracking reflector method at the spring equinox and autumnal equinox. Typically, in the local coordinate system, the solar elevation angle el' in the morning and afternoon of each day is higher than that at noon. The reflector has less occlusion and can receive more sunlight, so the optical efficiency vs. time curve is generally concave. The presence or absence of reflector tracking has the greatest impact on the optical efficiency in the morning and evening of the summer solstice. For fixed reflectors, due to the fixed tilt angle β of the reflector, to ensure the maximum energy output (priority capture of the sunlight at noon with high energy density), the cutoff rate η_2 in the morning and afternoon is lower than that at noon. Hence, the curve is convex. Due to the difference in the variation trend of the optical efficiency of each sub-item with time, the variation trend of the total optical efficiency with time in each typical day is different. Under the same reflector configuration, the efficiency of the summer solstice is the highest, followed by that of spring and autumn, and the winter solstice has the worst efficiency.

(6) Reflector energy efficiency η_{en}: according to Iqbal Model C and ASHRAE Model C [41], the direct solar radiation intensity (*DNI*) is approximately proportional to the solar

elevation angle, i.e., $DNI \propto \sin el$. Then, the energy weight of optical efficiency η_{sum} can be obtained as follows:

$$\eta_{en} = \eta_{sum} \times \frac{\sin el}{\sum_i \frac{\sin el_i}{n}} \tag{12}$$

Similar to the total optical efficiency η_{sum} of the reflector, the variation in η_{en} on four typical days with time is obtained, as shown in Figure 7.

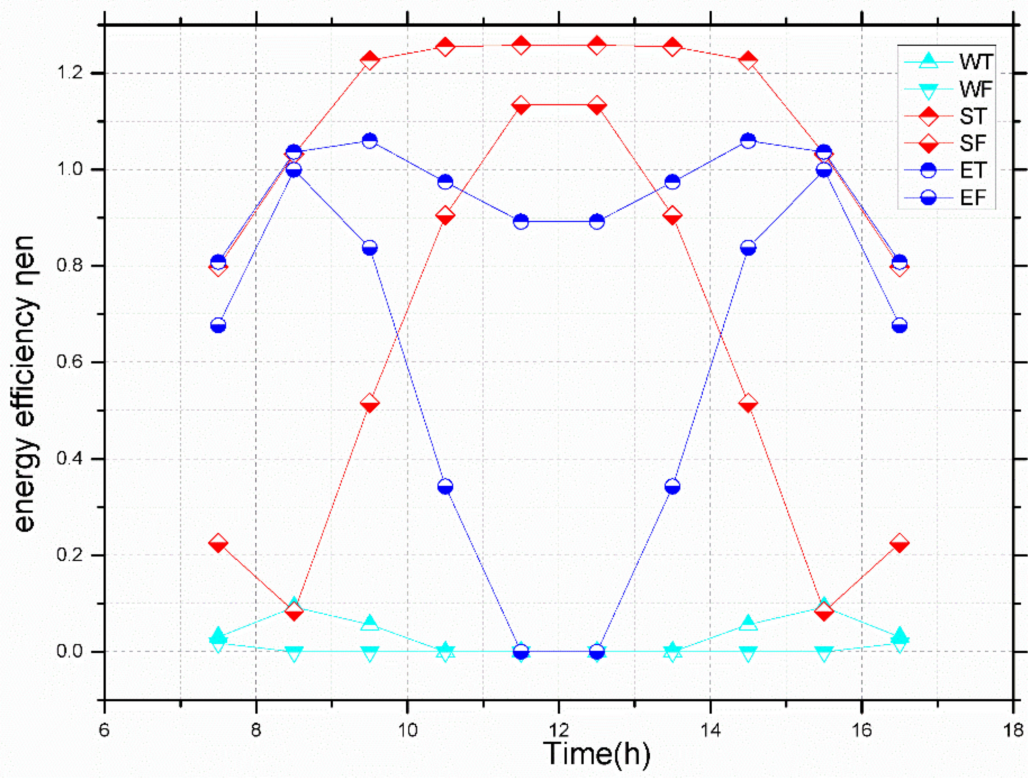

Figure 7. Variation in the reflector optical efficiency with time for the following parameter combination: φ = 37.5, α = 20°, h = 0.4 m, d = D = 1.74 m.

In Figure 7, the meaning of the labels is the same as that in Figure 6. Since the energy density of the sunlight is highest at noon, the total optical efficiency is weighted by energy, and the energy efficiency (η_{en}) curve rises near noon. Compared with the total optical efficiency curve, this curve is convex. η_{en} is greater than 1 at noon for the summer solstice. This is because the maximum solar elevation angle during the year is at noon for the summer solstice, and the corresponding solar irradiance is also the maximum, which may be much higher than the annual average value, so the energy weighting factor in this period is greater than 1.

3.3.5. Calculation of Total Solar Energy Absorbed by Module and Generated Power

The sunlight energy collected by the module for a given combination of structural parameters *(α, d, h)* is calculated.

Direct solar radiation intensity *DNI*:

$$DNI \times \sin(el) = GHI - DHI \tag{13}$$

Energy collected on the front:

$$E_{front} = BL \times \left(DNI \times sin\left(\alpha + el'\right) + DHI\right) \tag{14}$$

Energy scattered on the rear:

$$E_{rear\_1} = BL \times DHI \tag{15}$$

Supplemental light on the rear of the module:

$$E_{rear\_2} = Bl \times DNI \times \eta_{en} \tag{16}$$

Total solar radiant energy collected by the module:

$$E_{sum} = E_{rear\_1} + E_{rear\_2} + E_{front} \tag{17}$$

Total solar radiant energy collected by the module during the calculation time period

$$\kappa(\alpha,\ d,\ h) = \sum_{i}^{n} E_{sum}(T_i) \tag{18}$$

According to theoretical analysis, it is found that the total energy $\kappa(\alpha,\ d,\ h)\_year$ collected by the module annually is positively correlated with the variable d. Meanwhile, due to the limitation of the structural design conditions, the distance d between the reflector and module should not exceed the distance D between the modules. Therefore, in this paper, it is assumed that $d = D$.

Similarly, using the four typical days of spring equinox, autumnal equinox, summer solstice, and winter solstice as the calculation time points, under the parameter combination of $\varphi = 37.5$, $\alpha = 20°$, $h = 0.4$ m, $d = D = 1.74$ m, the variation in the total generated power of the system (E_{sum}) and the power generated by reflected light (E_{rear_2}) with time on four typical days are shown in Figures 8 and 9.

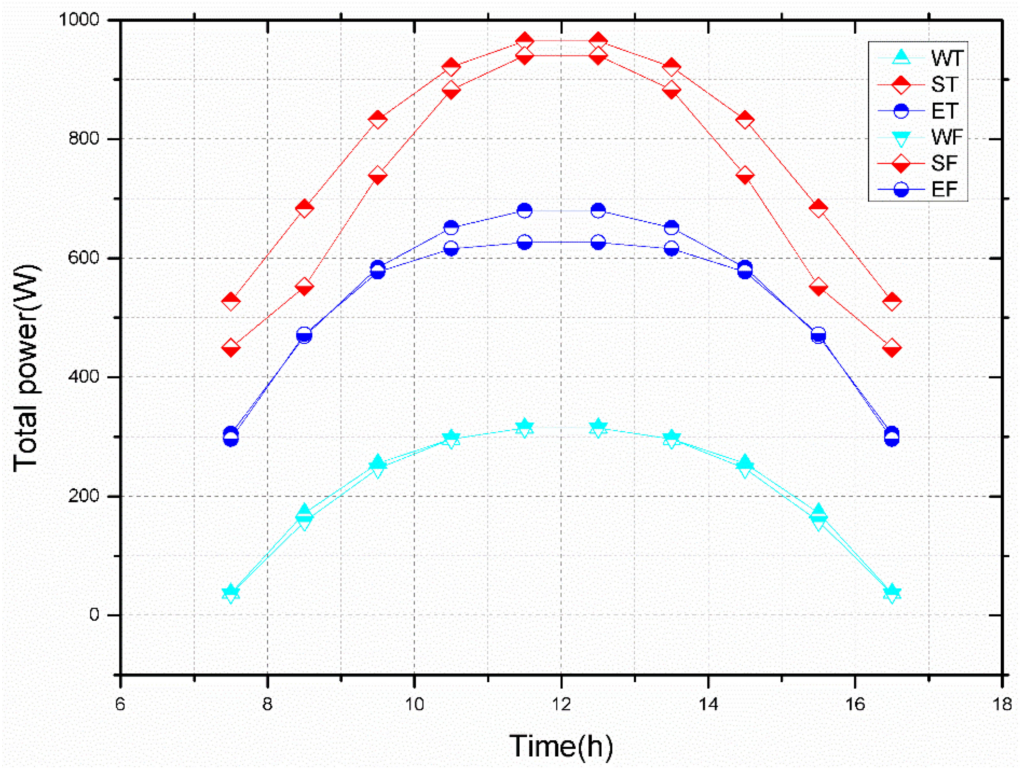

Figure 8. Variation in the total generated power E_{sum} of the single-module system with time.

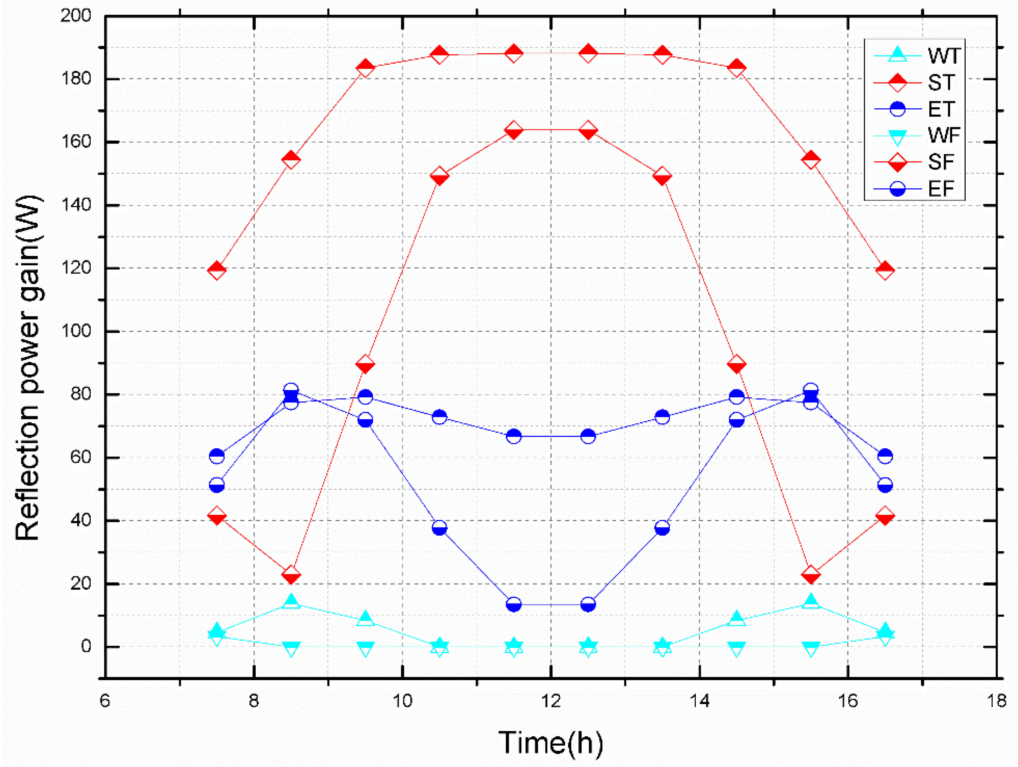

Figure 9. Variation in the power generated by reflected light (E_{rear_2}) of the single-module system with time.

In Figures 8 and 9, the meaning of labels is the same as that in Figure 6. The light supplementation and efficiency enhancement effect of the bifacial companion system is optimal at the summer solstice and the worst at the winter solstice. This is because the solar elevation angle decreases from summer solstice to winter solstice, so the amount of solar radiation that the reflector can receive between the modules is reduced, which in turn leads to a reduction in the amount of supplementary light on the rear of the module. Compared with fixed reflectors, tracking reflectors can effectively increase the power generation in the morning and afternoon periods at the summer solstice and winter solstice, and the effect is more pronounced during the summer solstice, and it can also increase the power generation during the noon period at the spring and autumnal equinox.

4. Case Study

4.1. Working Parameters

Six groups of different latitudes (φ in the range of 5–55°) and six groups of module tilt angles (α in the range of 5–55°,) are selected, and the reflector is set in tracking and fixed configurations to establish 72 sets of working conditions, which are shown in Table 2.

Table 2. Parameters for different working conditions.

Latitude φ at the Project Site	Module Tilt Angle α	Reflector Tilt Angle β
5°	5°	Fixed Tracking
15°	15°	
25°	25°	
35°	35°	
45°	45°	
55°	55	

4.2. Case Results

The optical parameters of the bifacial companion method for the above 72 sets of working conditions were optimized, and the annual average total power generation $\kappa(\alpha, d, h)\_year$ of optimized single-module system was calculated and compared with that of the horizontal single tracker with the optimal tilted bifacial module (HTTB). The results are shown in Figure 10.

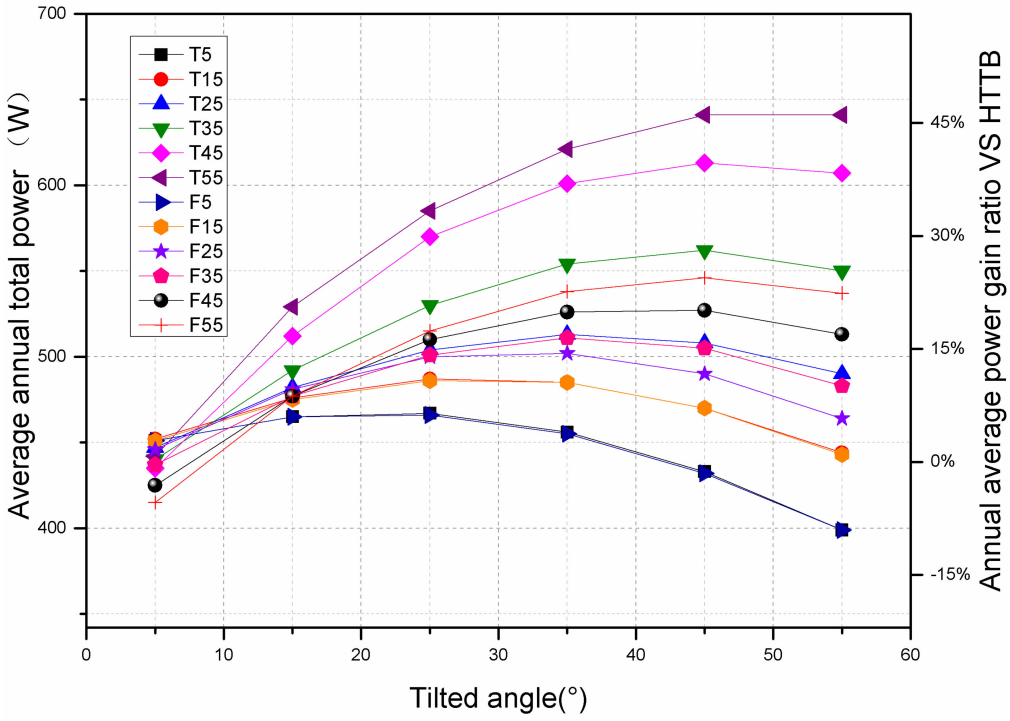

Figure 10. Comparison between total power generation $\kappa(\alpha, d, h)\_year$ of the optimal single-module system and horizontal single tracker with the optimal tilted bifacial module.

In Figure 10, the Y-axes on the left and right sides represent the annual average power generation of the bifacial companion single-component system and the gain ratio before and after adding the companion part, respectively. The label indicates the combination of reflector method and calculated latitude, where T—tracked, F—fixed. For example, T15 represents the maximum annual power generation of the tracking reflector single-module system in the 15° latitude area. The bifacial companion system has good application prospects in high latitude areas. Assuming that the solar radiation is the same everywhere and GHI = 2000 kW·h/m^2/year, the average power generation $\kappa(\alpha, d, h)\_year$ of the module on all sunny days in a year varies with the geographic latitude. At a geographic latitude of 55°, the average power of the module can reach 630 W. At high latitudes, comparing the annual average power generation $(\alpha, d, h)\_year$ of the bifacial companion system with that of the horizontal single tracker with the optimal tilted bifacial module, the gain of bifacial companion method is obvious. For latitudes above 35°, when the module tilt angle is 25°, the annual average power generation of the tracking reflector bifacial companion can be increased by more than 20%, and that of the fixed reflector bifacial companion can be increased by more than 13%. However, in low latitude areas, regardless of whether the reflector is tracking the Sun or not, the bifacial companion method has a minor effect on the increase in power generation: when the geographical latitude is 5°, the maximum increase is 3.5%, and when the geographical latitude is 15°, the maximum increase is 7.8%. The variation rule of the module tilt angle is to increase first and then decrease. In different latitude areas, the bifacial companion system has an optimal module tilt angle that maximizes the power generation efficiency of the single-module system. For the 37.5° latitude region, the optimal module tilt angles of the bifacial companion with

the tracking reflector and fixed reflector are 42° and 36°, respectively. The corresponding annual average power generation increase rates are 30% and 17%, respectively. When the module tilt angle is 20°, the annual power generation increase rates of the tracking and fixed methods are 25% and 15%, respectively. The optimal module tilt angles for each latitude are shown in Table 3.

Table 3. Theoretical optimal tilt angle of the bifacial companion system (°).

Latitude φ at the Project Site	Fixed Reflector	Tracking Reflector
5	15	15
15	25	25
25	30	36
37.5	36	42
45	40	47
55	41.5	50

5. Experimental Test

5.1. Test Methods

In Weihai (N 37.53° N, E 122.06° E, altitude 23 m, time zone UTC+8), a prototype of the fixed reflector bifacial companion system was tested. The ground environment was grassland, and the reflectance was 20–25%. The solar module selected for the test was LR5-72HBD 535 M, and the size of the module was 2256 × 1133 × 35 mm^3. The front power generation efficiency of the module was 20.9%, and the bifacial factor was 70 ± 5%. The selected test modules were located inside the photovoltaic array, and the positions inside the array were more representative.

The experiment was divided into three groups according to the module tilt angle (30°, 20°, 10°) for testing. Two modules were arranged at each angle. A reflector was arranged behind one of the modules, and the reflector was fixed on the bracket spindle at a fixed optimal tilt angle. Additionally, to ensure the synchronization of the test data and improve the test accuracy, two modules with the same angle were connected to the same microinverter (MI-1500, rated output power: 1500 W) during the test. Microinverters with more than 2 years of field experience were selected for the test, and the inverter power generation data showed a high degree of consistency over the years. Further, to prevent peak clipping, the cable channel with reflector was shunted and connected. At the same time, the power generation data and environmental data were monitored. In this study, relevant photovoltaic power data, sampled every 15 min, were selected, and the photovoltaic output power from 05:00 to 19:30 every day was selected for analysis. The test structure and wiring diagram are shown in Figure 11.

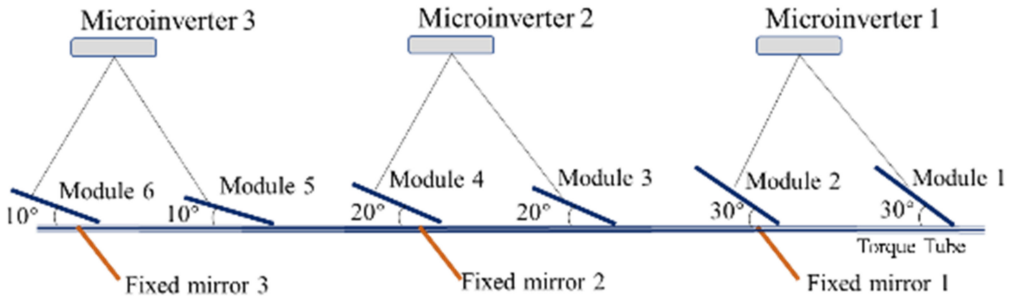

Figure 11. Test structure and wiring diagram.

Under three sets of tilt angles, the structural parameters of the test module and reflector arrangement are shown in Table 4. The prototype system used in the test is shown in Figure 12.

Table 4. Structural parameters and reflector arrangement for the test modules.

Serial Number of Test Module	Model Parameters					
	α (°)	d (m)	D (m)	h (m)	l (m)	β (°)
1, 2	30	1.96	1.96	0.46	0.87	37
3, 4	20	1.74	1.74	0.33	0.61	39
5, 6	10	1.46	1.46	0.21	0.39	41

Figure 12. Prototype system used in the test.

5.2. Test Results

The daily power generation of the prototype system was measured. Based on the test data of all sunny days during August and September 2021, a comparison between the daily power generation of each prototype system is given in Figures 13 and 14.

In Figure 14, the ordinate on the left is the measured daily power generation of the prototype, which corresponds to the histogram, and the ordinate on the right is the light gain ratio calculated based on the measured data, which corresponds to the red polyline.

As shown in Figures 13 and 14, the supplementary reflector light brings significant gain to the daily power generation of the prototype system. Among the 3 sets of prototype systems, the system with a 30° tilt angle has the largest daily power generation gain ratio, and the highest gain ratios in August and September are 18.1% and 3.7%, respectively. Further, the monthly average gain ratios in August and September are 14.06% and 9.7%, respectively. The maximum daily light gain ratios of the prototype system with a 20° tilt angle in August and September are 13% and 8.7%, respectively, and the monthly average gain ratios in August and September are 10.3% and 7.07%, respectively; the maximum daily light gain ratios of the prototype with a 10° tilt angle in August and September are 8.2% and 7%, respectively, and the monthly average gain ratios in August and September are 6.36% and 4.73%, respectively,

Additionally, there is a certain positive correlation between the gain ratio and daily power generation. This is because when the light resource is good, the proportion of direct solar radiation received by the reflector is higher, which is conducive to the reflection of light to the rear of the module.

The daily light gain ratio obtained by the test is compared with the theoretically calculated value in Figures 15 and 16.

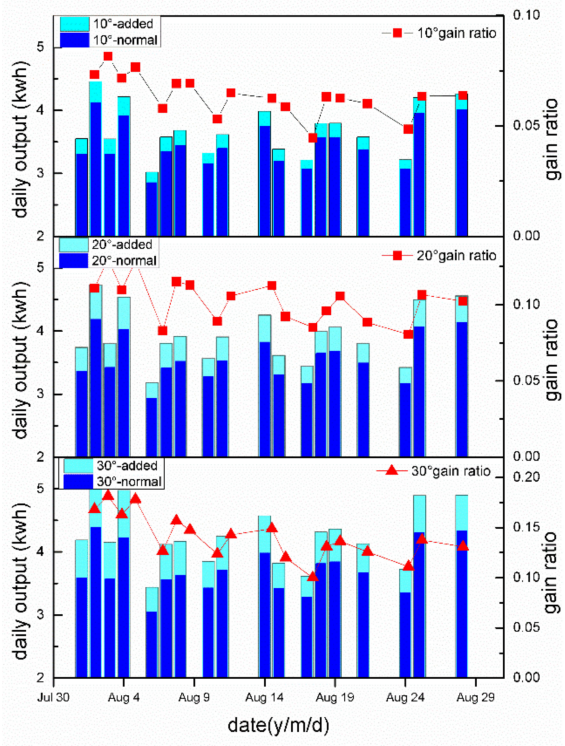

Figure 13. Comparison of the power generation and light gain of the prototype bifacial companion system in August before and after light supplementation.

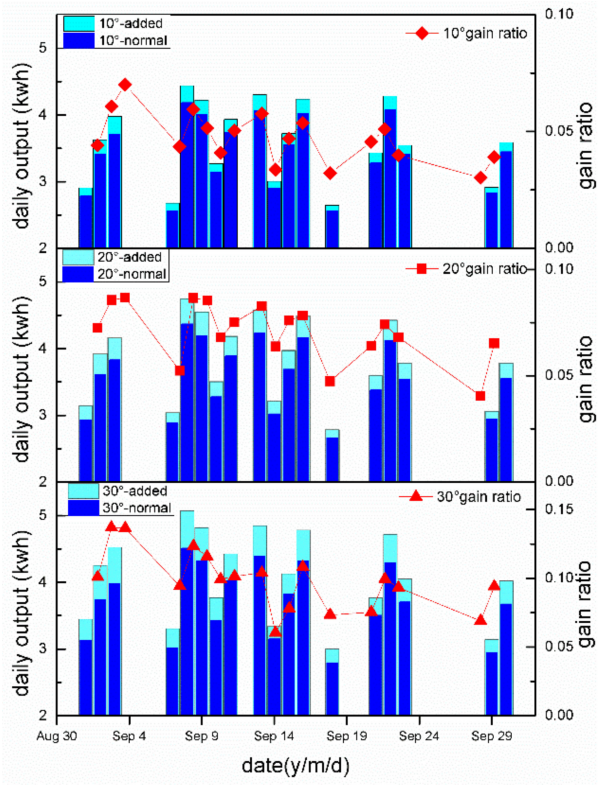

Figure 14. Comparison of the power generation and light gain of the prototype bifacial companion system in September before and after light supplementation.

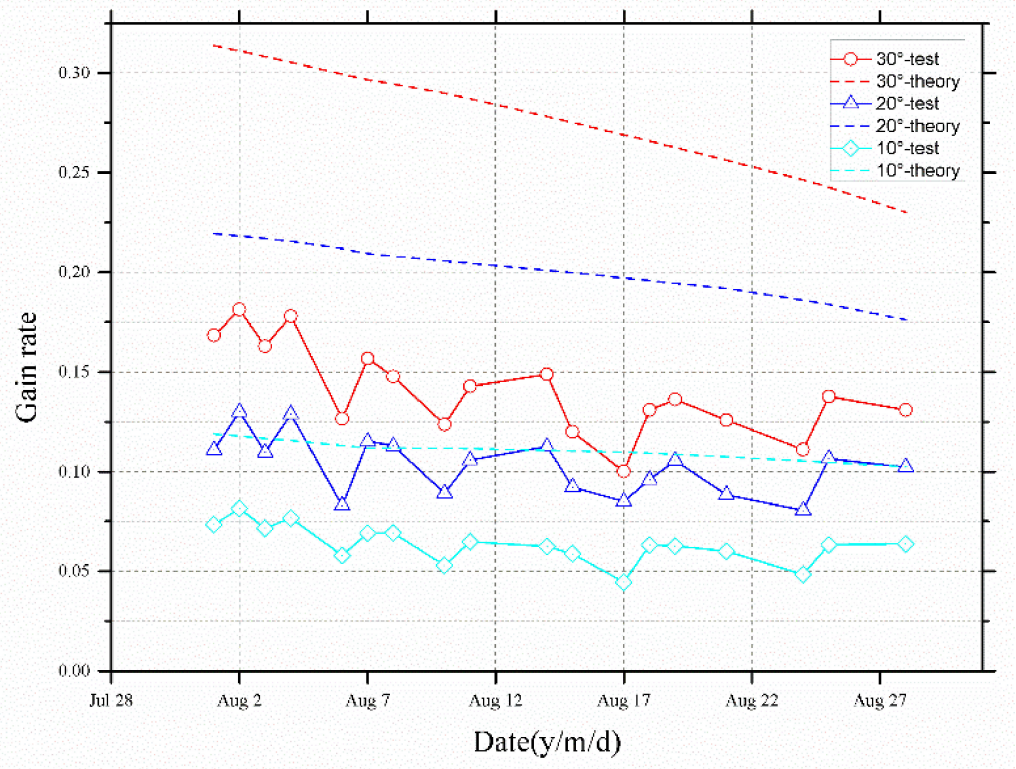

Figure 15. Test value vs. theoretical value of the daily gain ratio before and after light supplementation for the prototype system in August.

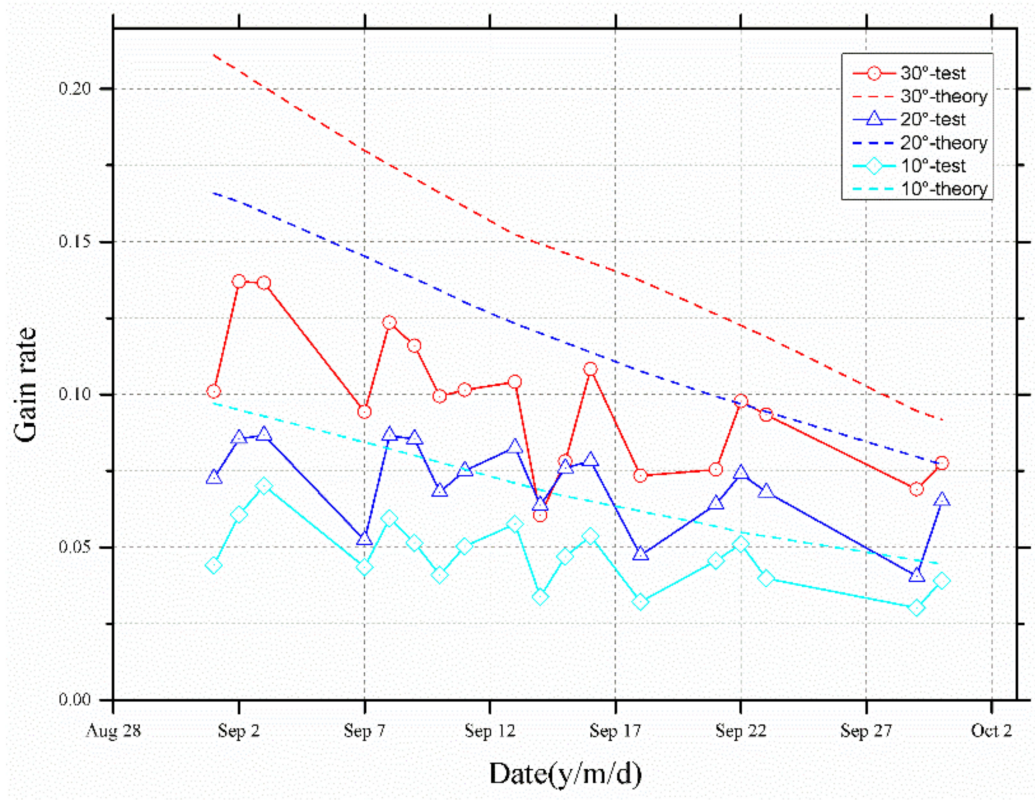

Figure 16. Test value vs. theoretical value of the daily gain ratio before and after light supplementation for the prototype system in September.

In Figures 15 and 16, the dotted line shows the theoretically calculated daily gain ratio of the ideal sunny day model. The black circle, blue triangle, and red diamond solid lines are the experimental test values of the daily gain ratio for the prototype systems with tilt angles of 30°, 20°, and 10°, respectively. The theoretical value of daily gain is based on an ideal sunny day, where it is assumed that the structural and transmission error is the limit value of 0. If the variability of the weather during the day and the actual error in the prototype production are taken into account, the test value of the daily gain ratio can fluctuate to a certain extent. Therefore, the test value is less than the theoretical value. However, the overall variation trend of the theoretical and test values is basically the same, and both show a gradually decreasing trend with time from August. This is because the solar elevation angle decreases with the passage of the season, so the amount of usable solar radiation received by the reflector is reduced, which in turn reduces the amount of light supplemented on the rear side of the module.

5.3. Uncertainty Analysis of Test Data

The test data in this paper corresponds to the daily average power generation data on all sunny days in August and September 2021. However, the cloud blocking conditions that may occur during sunny days or the sunlight scattering conditions caused by high air humidity can reduce the proportion of direct light received by the bifacial companion's mirror system. This in turn can weaken the system's effect on power generation gain to a certain extent.

In addition, the solar tracking error as well as the geometrical manufacturing error of the prototype can adversely affect the test results.

6. Economic Evaluation of the Scheme

The economic evaluation of the scheme is conducted by using the levelized cost of energy (LCOE) of the newly added system (supplementary light system). First, the total cost in the design life is estimated, and it is converted into the cost per kilowatt hour, according to the expected total power generation. To evaluate the economic value of the scheme, Table 5 shows the estimated cost of the tracking mirror scheme as an example, where the annual solar energy is set as 2000 kWh/m^2/year, the annual power generation time is 2000 h/year, and the designed service life is 25 years. The module is LR5-72HBD 535 M with a size of 2256 mm × 1133 mm × 35 mm. The power generation rate of the companion is ~30%. It can be seen from Table 5 that the LCOE for the companion part of the bifacial companion method is 0.0038–0.0054 $/kWh (the cost in Table 5 is based on the Chinese market materials and labor market conditions in 2021), which is far lower than that for the traditional horizontal single-axis tracker (~0.05 $/kWh). This verifies that the bifacial companion solution is more cost-effective than the traditional solution.

Table 5. Cost analysis of the bifacial companion method.

Cost of Bifacial Companion Method (Supplementary Light System) ($/25 Years)		
Reflector (super white float glass)	Production cost	8–12
	Operation and maintenance costs (cleaning)	8–10
Tracking system (push rod linkage mechanism, accuracy ±3°)	Cost of production	3–5
	Operation and maintenance costs (wear and energy consumption)	8–10
Mirror holder	Cost of production	4–6
Total	——	31–43
Expected total power generated per module (kWh/25 years)	26750	
Total expected incremental power generation by the companion system (kWh/25 years)	8025	
Companion kWh cost ($/kWh)	0.0039–0.0054	
LCOE of traditional flat order tracking system ($/kWh)	~0.05	

7. Conclusions

The bifacial companion method was proposed for the efficiency enhancement of tilted bifacial modules with a horizontal single-axis tracker. Through theoretical calculations and field experimental tests, the technical feasibility of the proposed method was verified from two aspects. The bifacial companion method effectively improved the power generation efficiency on the rear side, maximized the power generation potential, and reduced the cost of bifacial photovoltaic module, which provides a technically and economically viable direction for the development of photovoltaic support industry. The main results of the study are summarized as follows:

(1) The power generation efficiency of the bifacial companion system can be higher than that of any existing photovoltaic support form. As an optical component sensitive to the structural size, the calculation process to obtain the optimal parameter combination (α, β, D, d, l, h) of the bifacial companion system under the known project site and characteristic parameters of the photovoltaic module was described.

(2) The bifacial companion method was found to be particularly suitable for applications in mid-to-high latitudes. The higher the latitude, the greater the increase rate of system power generation, and reflector tracking was more conducive to improving the power generation efficiency of the system. In project sites with different latitudes, an optimal module tilt angle existed that maximized the efficiency. The closer the module angle to the optimal tilt angle, the higher the power generation efficiency of the system. Meanwhile, compared to the fixed solar reflector, the tracking solar reflector was more conducive to improving the power generation efficiency of the system. For the 37.5° latitude area, the annual average power generation gain ratio of the bifacial companion system with the tracking reflector and fixed reflector could reach up to 30% and 17%, respectively.

(3) In Weihai (37.53° N, 122.06° E), the experimental test results reveal that for the three sets of bifacial companion prototype systems with a fixed reflector (module tilt angles of 30°, 20°, and 10°), the maximum gain ratios of daily power generation in August 2021 are 18.1%, 13% and 8.2%, respectively; the maximum gain ratios of daily power generation in September 2021 are 13.7%, 8.7% and 7%, respectively, and the test data is consistent with the theoretical results.

(4) According to the cost analysis, compared with the traditional solution, the bifacial companion solution based on the horizontal single-axis tracker with inclination angle is more cost-effective and can significantly reduce the cost of electricity.

8. Future Prospects

The following aspects will be considered in future studies:

(1) A comparative analysis of different parameters, including economic efficiency, between the bifacial companion tracking mirror prototype and the horizontal single-axis tracker with tilted module will be conducted.

(2) Based on the series-parallel characteristics of the module wafers, the uniformity of the reflected light distribution received at the back of the module can be improved.

(3) As an extension of the bifacial companion method, for other existing mature stent technologies, such as horizontal single-axis tracker, the backside light supplementation methods will be examined.

Author Contributions: Conceptualization, S.W.; methodology, S.W., J.Z. and Y.S.; validation, S.W., C.L. and J.Z.; formal analysis, S.W., J.Z. and L.M.; investigation, S.W., L.M. and J.Z.; supervision, Y.S. and C.L.; writing—original draft preparation, S.W.; writing—review and editing, Y.S., C.L. and L.M. All authors have read and agreed to the published version of the manuscript.

Funding: This research received no external funding.

Institutional Review Board Statement: Not applicable.

Informed Consent Statement: Not applicable.

Data Availability Statement: Not applicable.

Conflicts of Interest: The authors declare no conflict of interest.

References

1. Venkateswari, R.; Sreejith, S. Factors influencing the efficiency of photovoltaic system. *Renew. Sustain. Energy Rev.* **2019**, *101*, 376–394. [CrossRef]
2. Yusufoglu, U.A.; Pletzer, T.M.; Koduvelikulathu, L.J.; Comparotto, C.; Kopecek, R.; Kurz, H. Analysis of the Annual Performance of Bifacial Modules and Optimization Methods. *IEEE J. Photovolt.* **2015**, *5*, 320–328. [CrossRef]
3. Sun, X.; Khan, M.R.; Deline, C.; Alam, M.A. Optimization and performance of bifacial solar modules: A global perspective. *Appl. Energy* **2018**, *212*, 1601–1610. [CrossRef]
4. Guerrero-Lemus, R.; Vega, R.; Kim, T.; Kimm, A.; Shephard, L. Bifacial solar photovoltaics—A technology review. *Renew. Sustain. Energy Rev.* **2016**, *60*, 1533–1549. [CrossRef]
5. Gu, W.; Ma, T.; Ahmed, S.; Zhang, Y.; Peng, J. A comprehensive review and outlook of bifacial photovoltaic (bPV) technology. *Energy Convers. Manag.* **2020**, *223*, 113283. [CrossRef]
6. Kopecek, R.; Libal, J. Bifacial Photovoltaics 2021: Status, Opportunities and Challenges. *Energies* **2021**, *14*, 2076. [CrossRef]
7. Shen, L.T.; Pravettoni, M.; Deline, C.; Stein, J.S.; Kopecek, R.; Singh, J.P.; Luo, W.; Wang, Y.; Aberle, A.G.; Khoo, Y.S. A review of crystalline silicon bifacial photovoltaic performance characterization and simulation. *Energy Environ. Sci.* **2019**, *12*, 116–148. [CrossRef]
8. Yu, B.; Song, D.; Sun, Z.; Liu, K.; Zhang, Y.; Rong, D.; Liu, L. A study on electrical performance of N-type bifacial PV modules. *Sol. Energy* **2016**, *137*, 129–133. [CrossRef]
9. Zhang, C.; Shen, H.; Sun, L.; Yang, J.; Wu, S.; Lu, Z. Bifacial p-Type PERC Solar Cell with Efficiency over 22% Using Laser Doped Selective Emitter. *Energies* **2020**, *13*, 1388. [CrossRef]
10. Rohatgi, A.; Meier, D.L.; McPherson, B.; Ok, Y.-W.; Upadhyaya, A.D.; Lai, J.-H.; Zimbardi, F. High-Throughput Ion-Implantation for Low-Cost High-Efficiency Silicon Solar Cells. *Energy Procedia* **2012**, *15*, 10–19. [CrossRef]
11. Reininghaus, N.; Feser, C.; Hanke, B.; Vehse, M.; Agert, C. Amorphous single-junction cells for vertical BIPV application with high bifaciality. *Energy Sci. Eng.* **2016**, *4*, 183–189. [CrossRef]
12. Urrejola, E.; Valencia, F.; Vidal, E.L.F.; Deline, C.; Pelaez, S.A.; Meydbray, J.; Clifford, T.; Kopecek, R.; Stein, J.S. BifiPV2020 Bifacial Workshop: A Technology Overview. NREL Summary of bifiPV2020. Available online: https://www.nrel.gov/docs/fy21osti/77817.pdf (accessed on 22 October 2020).
13. Podlowski, L. White Paper on Bifacial PV. PI Photovoltaik-Institut Berlin AG. Available online: https://www.pi-berlin.com/wp-content/uploads/2019/10/White-Paper-Bifacial-PV-Technology-PI-Berlin.pdf (accessed on 25 October 2019).
14. Al-Mohamad, A. Efficiency improvements of photo-voltaic panels using a Sun-tracking system. *Appl. Energy* **2004**, *79*, 345–354. [CrossRef]
15. Lazaroiu, G.C.; Longo, M.; Roscia, M.; Pagano, M. Comparative analysis of fixed and sun tracking low power PV systems considering energy consumption. *Energy Convers. Manag.* **2015**, *92*, 143–148. [CrossRef]
16. Singh, R.; Kumar, S.; Gehlot, A.; Pachauri, R. An imperative role of sun trackers in photovoltaic technology: A review. *Renew. Sustain. Energy Rev.* **2018**, *82*, 3263–3278. [CrossRef]
17. Patel, M.T.; Ahmed, M.S.; Imran, H.; Butt, N.Z.; Khan, M.R.; Alam, M.A. Global analysis of next-generation utility-scale PV: Tracking bifacial solar farms. *Appl. Energy* **2021**, *290*, 116478. [CrossRef]
18. Nsengiyumva, W.; Chen, S.G.; Hu, L.; Chen, X. Recent advancements and challenges in Solar Tracking Systems (STS): A review. *Renew. Sustain. Energy Rev.* **2018**, *81*, 250–279. [CrossRef]
19. Hafez, A.Z.; Yousef, A.M.; Harag, N.M. Solar tracking systems: Technologies and trackers drive types—A review. *Renew. Sustain. Energy Rev.* **2018**, *91*, 754–782. [CrossRef]
20. Awasthi, A.; Shukla, A.K.; Murali Manohar, S.R.; Dondariya, C.; Shukla, K.N.; Porwal, D.; Richhariya, G. Review on sun tracking technology in solar PV system. *Energy Rep.* **2020**, *6*, 392–405. [CrossRef]
21. Khan, M.R.; Patel, M.T.; Asadpour, R.; Imran, H.; Butt, N.Z.; Alam, M.A. A review of next generation bifacial solar farms: Predictive modeling of energy yield, economics, and reliability. *J. Phys. D Appl. Phys.* **2021**, *54*, 323001. [CrossRef]
22. Mousazadeh, H.; Keyhani, A.; Javadi, A.; Mobli, H.; Abrinia, K.; Sharifi, A. A review of principle and sun-tracking methods for maximizing solar systems output. *Renew. Sustain. Energy Rev.* **2009**, *13*, 1800–1818. [CrossRef]
23. Clifford, M.; Eastwood, D. Design of a novel passive solar tracker. *Sol. Energy* **2004**, *77*, 269–280. [CrossRef]
24. Fathabadi, H. Novel high efficient offline sensorless dual-axis solar tracker for using in photovoltaic systems and solar concentrators. *Renew. Energy* **2016**, *95*, 485–494. [CrossRef]
25. Fathabadi, H. Novel high accurate sensorless dual-axis solar tracking system controlled by maximum power point tracking unit of photovoltaic systems. *Appl. Energy* **2016**, *173*, 448–459. [CrossRef]
26. Egido, M.A.; Lorenzo, E. Bifacial Photovoltaic Panels with Sun Tracking. *Int. J. Sol. Energy* **1986**, *4*, 97–107. [CrossRef]
27. Gu, W.; Li, S.; Liu, X.; Chen, Z.; Zhang, X.; Ma, T. Experimental investigation of the bifacial photovoltaic module under real conditions. *Renew. Energy* **2020**, *173*, 1111–1122. [CrossRef]

28. Pelaez, S.A.; Deline, C.; Greenberg, P.; Stein, J.S.; Kostuk, R.K. Model and Validation of Single-Axis Tracking with Bifacial PV. *Int. J. Sol. Energy* **2019**, *9*, 715–721. [CrossRef]
29. Madala, S.; Boehm, R.F. A review of nonimaging solar concentrators for stationary and passive tracking applications. *Renew. Sustain. Energy Rev.* **2017**, *71*, 309–322. [CrossRef]
30. Cuevas, A.; Luque, A.; Eguren, J.; Alamo, J.D. 50 percent more output power from an albedo collecting flat panel using bifacial solar cells. *Sol. Energy* **1982**, *29*, 419–420. [CrossRef]
31. Al-Shohani, W.A.; Al-Dadah, R.; Mahmoud, S.; Algareu, A. Optimum design of V-trough concentrator for photovoltaic applications. *Sol. Energy* **2016**, *140*, 241–254. [CrossRef]
32. Maiti, S.; Banerjee, S.; Vyas, K.; Patel, P.; Ghosh, P.K. Self regulation of photovoltaic module temperature in V-trough using a metal–wax composite phase change matrix. *Sol. Energy* **2011**, *85*, 1805–1816. [CrossRef]
33. Tina, G.; Scandura, P. Case study of a grid connected with a battery photovoltaic system: V-trough concentration vs. single-axis tracking. *Energy Convers. Manag.* **2012**, *64*, 569–578. [CrossRef]
34. Ooshaksaraei, P.; Sopian, K.; Zulkifli, R.; Alghoul, M.; Zaidi, S.H. Characterization of a Bifacial Photovoltaic Panel Integrated with External Diffuse and Semimirror Type Reflectors. *Int. J. Photoenergy* **2013**, *2013*, 465837. [CrossRef]
35. Guo, S.; Walsh, T.M.; Peters, I.M. Vertically mounted bifacial photovoltaic modules: A global analysis. *Energy* **2013**, *61*, 447–454. [CrossRef]
36. Chudinzow, D.; Klenk, M.; Eltrop, L. Impact of field design and location on the techno-economic performance of fixed-tilt and single-axis tracked bifacial photovoltaic power plants. *Sol. Energy* **2020**, *207*, 564–578. [CrossRef]
37. Patel, M.T.; Khan, M.; Sun, X.; Alam, M.A. A worldwide cost-based design and optimization of tilted bifacial solar farms. *Appl. Energy* **2019**, *247*, 467–479. [CrossRef]
38. Riedel-Lyngskær, N.; Poulsen, P.B.; Jakobsen, M.L.; Nørgaard, P.; Vedde, J. Value of bifacial photovoltaics used with highly reflective ground materials on single-axis trackers and fixed-tilt systems: A Danish case study. *IET Renew. Power Gener.* **2021**, *14*, 3946–3953. [CrossRef]
39. Wong, L.T.; Chow, W.K. Solar radiation model. *Appl. Energy* **2001**, *69*, 191–224. [CrossRef]
40. Longi LR5-72HBD 525-545M Datasheet. Available online: https://en.longi-solar.com/home/products/Hi_MO5.html (accessed on 12 May 2021).
41. De Melo, K.B.; Moreira, H.S.; Villalva, M.G. Influence of Solar Position Calculation Methods Applied to Horizontal Single-Axis Solar Trackers on Energy Generation. *Energies* **2020**, *13*, 3826. [CrossRef]